



## Time-Dependent Bias in Instantaneous Ceptometry Caused by Row Orientation

William T. Salter, Matthew E. Gilbert, and Thomas N. Buckley\*

### Core Ideas

- Time of day can strongly bias inferences based on instantaneous ceptometry.
- This bias is caused by interaction of solar zenith angle and row orientation.
- Continuously recording ceptometers could be used to avoid time-dependent bias.
- We detail how to build high-accuracy low-cost continuously recording ceptometers.
- These could be used to develop correction factors for instantaneous measurements.

Ceptometry (the measurement of average photosynthetically active radiation under a plant canopy using many individual light sensors connected in parallel on a long bar) is commonly used to infer canopy light interception as well as leaf area index. Typically, the user places a ceptometer below the canopy and records a measurement, which is compared with a concurrent above-canopy measurement to produce a value of transmittance and then corrected for the effects of solar zenith and solar beam fraction. In row crops, canopy architecture is often systematically clumped in ways that may bias inferences based on ceptometer measurements. The role of spatial sampling in bias due to clumping has been extensively studied in the literature, but time-dependent bias has not. We assessed this bias using 68 handmade continuously recording ceptometers in 239 wheat (*Triticum aestivum* L.) genotypes in Australia and made confirmatory measurements in California. We found that canopy properties inferred from instantaneous ceptometry varied widely, both randomly and systematically in time, when compared with properties inferred from continuous measurements. However, these biases tended to be somewhat similar across genotypes on a given day, arising from the interaction of solar zenith and non-random features of the canopy distribution caused by row planting. We recommend that continuous ceptometry be used in conjunction with instantaneous ceptometry to correct for these biases, and we provide schematics for low-cost handmade ceptometers.

W.T. Salter, School of Life and Environmental Sciences, Sydney Institute of Agriculture, Univ. of Sydney, Brownlow Hill, NSW 2570, Australia; M.E. Gilbert and T.N. Buckley, Dep. of Plant Sciences, Univ. of California, Davis, CA 95616.

Copyright © American Society of Agronomy and Crop Science Society of America. 5585 Guilford Rd., Madison, WI 53711 USA. This is an open access article distributed under the CC BY license (<https://creativecommons.org/licenses/by/4.0/>).  
Plant Phenome J. 1: 180004 (2017)  
doi:10.2135/tppj2018.07.0004

Received 13 July 2018.

Accepted 16 Oct. 2018.

Supplemental material online.

\*Corresponding author (tnbuckley@ucdavis.edu)

Ceptometers are linear arrays of light sensors used to quantify the average light intensity under plant canopies for the purpose estimating canopy light interception and leaf area index or biomass (e.g., Armbrust, 1990; Pearcy et al., 1990; Welles, 1990; Rosenthal and Gerik, 1991; Grossman and DeJong, 1998; Whaley et al., 2000; Francone et al., 2014). Because ceptometer measurements are fairly straightforward and rapid, ceptometry is widely used for phenotyping row crops in agricultural research (for example, a Google Scholar search for *ceptometer* and *crop* between 2007 and 2017 produced 1950 results). The principle of ceptometry is simple: canopy transmittance ( $\tau$ , the ratio of photosynthetically active radiation, PAR, below the canopy to that above the canopy) is strongly dependent on the surface area of light-absorbing materials within the canopy, so PAR measurements above and below the canopy can be used to estimate the leaf area index (LAI) or more generally the plant area index (PAI, which includes stems, culms, and reproductive structures). In limiting cases (e.g., when all radiation is diffuse), PAI is directly proportional to the logarithm of  $1/\tau$  (Lang and Xiang, 1986). More realistically, the relationship of PAI to  $\tau$  depends on the beam fraction of incoming PAR ( $f_b$ ), the leaf absorptance ( $a$ ), and the effective canopy extinction coefficient ( $K$ );  $K$  in turn depends on the solar zenith ( $\theta$ , the angle of the sun below a point directly overhead) and the leaf angle distribution. These effects can be modeled, enabling inference of PAI from  $\tau$  (Campbell, 1986; Armbrust, 1990; Campbell and Van Evert, 1994; Cohen et al., 1997; Decagon Devices, 2017).

Abbreviations: LAI, leaf area index; PAI, plant area index; PAR, photosynthetic active radiation; PPFD, photosynthetic photon flux density.

Like any optical method for quantifying plant canopy properties, ceptometry is subject to potential sampling biases and errors due to spatial variability in canopy properties (“clumping”). Much research has thus addressed how clumping affects the inference of PAI from ceptometry and other optical methods (Fassnacht et al., 1994; Chen and Cihlar, 1995; Chen et al., 1997; Cohen et al., 1997; White et al., 1997, 2000; Kucharik et al., 1998, 1999; Johnson et al., 2010).

The time of measurement can also bias measurement of  $\tau$  by ceptometry, and inference of PAI from  $\tau$ , due to the interaction of spatial aggregation with solar position. This is particularly significant in row crops, where clumping is highly anisotropic: Fuchs and Stanhill (1980) modeled light interception in row crops and showed that light interception should increase as the solar zenith angle ( $\theta$ ) increases (i.e., as solar elevation decreases, such as toward the shoulders of the day) and as the angle  $\phi$  between the solar azimuth and the row orientation increases (i.e., as the solar beam is farther from parallel to the rows) (Fig. 1 illustrates the meanings of  $\theta$  and  $\phi$ ). However, the effect of  $\phi$  on ceptometer measurements has been largely overlooked (but see López-Lozano et al., 2009; López-Lozano and Casterad, 2013). Advice regarding the application of ceptometry in row crops (e.g., Pask et al., 2012; Webb et al., 2016; Decacon Devices, 2017) emphasizes spatial sampling both within and between planting rows but does not address the effect of row orientation in relation to solar azimuth other than tacitly, e.g., by recommending that measurements be made during a period of several hours near solar noon (e.g., 1100–1400 h, CIMMYT; solar noon  $\pm$  3 h, Delta-T Devices). It is unclear whether such measurement windows are sufficiently narrow

to avoid bias due to shifts in  $\phi$ . Any effect of  $\phi$  on ceptometer readings could, in principle, be addressed by leaving ceptometers in place beneath the canopy for an entire day. However, the high cost of commercial ceptometers has made this approach impractical for use in phenotyping large numbers of field plots.

The objectives of this study were twofold: first, to assess the potential impact of the diurnal variation in  $\phi$  (solar alignment with crop planting rows) on PAI inferred from instantaneous ceptometer measurements by placing continuously recording ceptometers beneath wheat canopies, and second, to provide a resolution to  $\phi$ -related ceptometer bias by demonstrating how continuously recording ceptometers of high accuracy can be built by hand at low cost. We placed 68 handmade 1-m ceptometers (PARbars) beneath canopies of 239 genotypes of row-planted wheat in Australia and recorded at least one diurnal cycle of transmittance and inferred PAI for each plot. We made confirmatory measurements in California using contrasting row orientations, planting densities, and weather conditions.

## Materials and Methods

### Ceptometer Construction

Each PARbar ceptometer consists of 50 photodiodes (EAALSDSY6444A0, Everlight Americas) connected in parallel, providing an integrated reading of PAR (wavelength range  $\lambda$  400–700 nm) across a 1-m length. The PARbars were constructed using readily available parts and non-specialist tools (Supplemental Table S1). Fifty photodiodes are mounted onto the underside of an acrylic diffuser bar (1200-mm length by

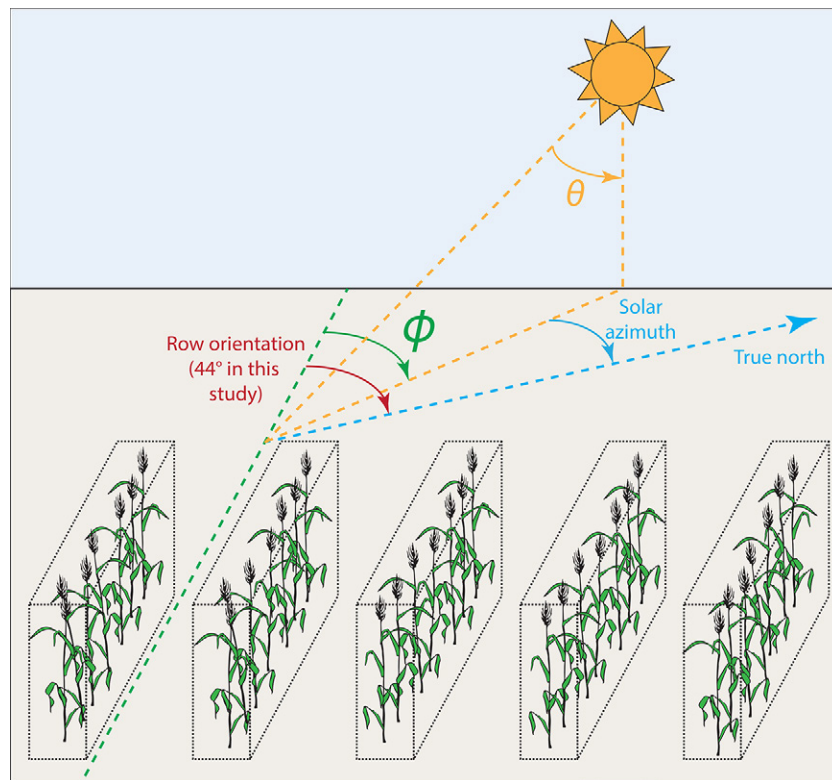


Fig. 1. Diagram illustrating solar zenith angle ( $\theta$ , the complement of solar elevation angle) and the angle  $\phi$  between the solar azimuth and the row orientation. The rows planted in the Australian portion of the study had an orientation of  $44^\circ$  (west of true north).

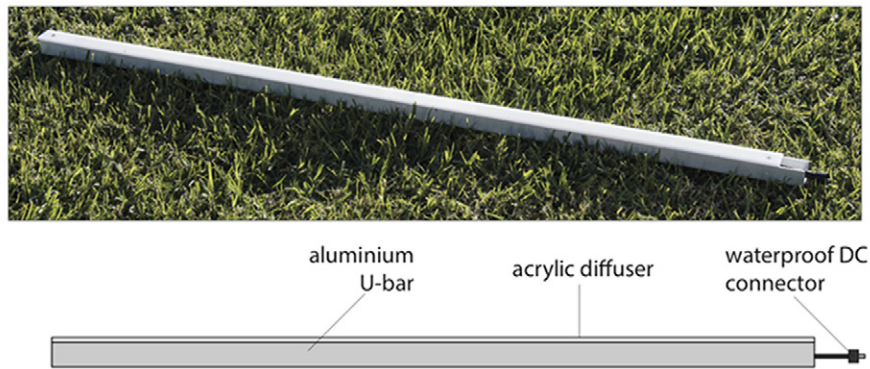
30-mm width by 4.5-mm thickness, 445 Opal White, Plastix Australia Pty. Ltd.) at 2-cm intervals using super glue. Each photodiode contact is soldered onto a length of bare copper wire. Every solder connection is tested by consecutively shining a light onto individual photodiodes and checking for a voltage signal. A waterproof direct current (DC) connector (ADA743, Core Electronics) is soldered to the copper wires to allow disconnection from the datalogger when not in use. The electronics are then encased in epoxy (651 Universal Epoxy Potting Resin, Solid Solutions) for waterproofing. The acrylic bar is then attached to an aluminum U-bar for rigidity, using bolts and predrilled, pre-threaded holes. Finally, polyurethane foam filler is injected into the U-bar to secure the diffuser to the aluminum across the entire 1-m length. Figure 2 illustrates the arrangement of PARbar components, as well as an example of a completed unit. The PARbars used in California were similar in construction but used 40 photodiodes, were 91 cm long, and used Sign Lighting

White 40% transmission Chemcast acrylic (TAP Plastics) as a diffuser.

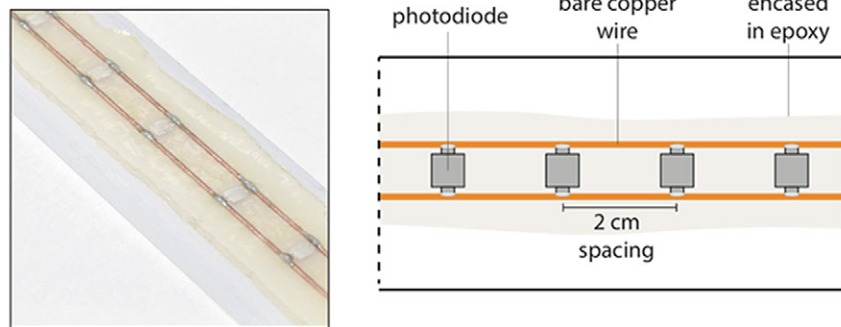
The photodiodes used in the PARbars are sensitive between wavelengths of 390 and 700 nm, with very little response outside this waveband (Supplemental Fig. S1). This allows them to be used without the need for costly filters. They can also operate across a large temperature range ( $-40$  to  $80^{\circ}\text{C}$ ). The photodiodes were connected in parallel with a  $1.5\ \Omega$  (Australia) or  $10\ \Omega$  (California) shunt resistor, producing a linear quantum response (Fig. 3). We used low-temperature-coefficient precision resistors to prevent shifts in ambient temperature from influencing the voltage signal for a given light level.

The PARbars were individually calibrated using a quantum sensor (Li-190R, LI-COR Biosciences) immediately before deployment in the field. In Australia, calibration was performed outside under clear skies, using shade cloth to successively reduce the light level to produce a four-point calibration curve spanning 0 to  $1500\ \mu\text{mol photons m}^{-2}\ \text{s}^{-1}$ . The dark calibration point was

### Complete PARbar



### Underside of acrylic diffuser



### Circuit diagram

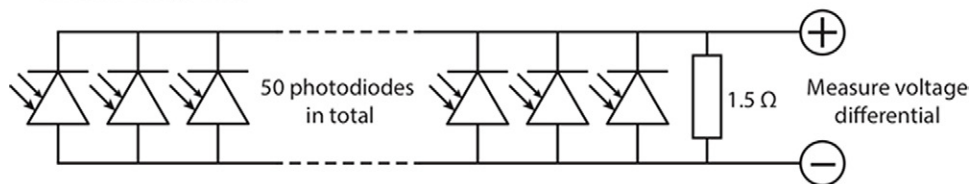


Fig. 2. Illustration of PARbar handmade ceptometers: photo and illustration of complete PARbar; cable connection is at right (top); photo (middle left) and diagram (middle right) of diode and wire mounting on the inner face of the diffuser bar that forms the top of the PARbar; and circuit diagram showing electrical connections, where each triangle represents a photodiode, and the “ $1.5\ \Omega$ ” object is a low-temperature coefficient  $1.5\text{-}\Omega$  resistor (bottom).

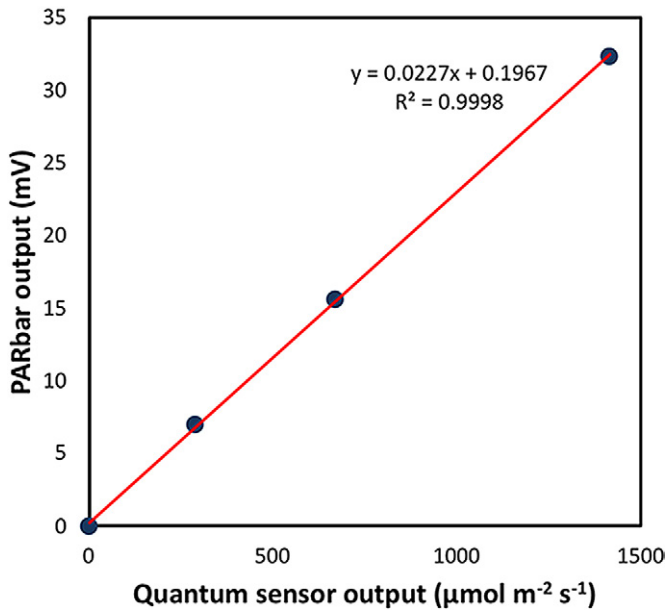


Fig. 3. Relationship between differential voltage output of a PARbar and that of a LI-COR Li-190R quantum sensor.

measured inside under complete darkness. In California, calibrations were done by maintaining the PARbars above the canopy for a diurnal cycle. Each PARbar's output was converted to photosynthetic photon flux density (PPFD) using that PARbar's individual calibration.

### Field Setup: Australia

Wheat was planted in the field in Narrabri, NSW, Australia ( $30^{\circ}19'0''$  S  $149^{\circ}46'0''$  E) in May 2017 and measurements taken during a 2-wk period in September 2017. Wheat was planted in 2- by 6-m plots, with five sowing rows in each plot. Plots were oriented with rows running northwest to southeast, at an angle of  $44^{\circ}$  west relative to true north (Fig. 1). Two weeks before measurements began, access lanes were mowed between ranges of plots, leaving each plot 2 by 4 m in size for measurement and later harvest. Two to three buffer rows and ranges were planted at the outer margin of the planting area. A total of 239 genotypes were planted, with two plots per genotype (the genotypes are described below). One set of 239 plots (one plot per genotype) were planted in a block of 17 rows and 16 ranges, including one range (17 rows) of buffer between and two groups of eight and seven ranges; another 239 plots (a second replicate for each genotype) were planted in an adjacent block immediately southeast. Genotypes were randomly distributed within each block. Phenological development was unusually quick due to dry and warm conditions. The distribution of phenological stages across the measurement campaign is shown in Supplemental Fig. S2; the median Zadoks growth stages (Zadoks et al., 1974) were 59 (ear emergence complete) and 65 (anthesis half-way) for the first and second blocks of replicate plots for each genotype, measured on 3 to 10 and 11 to 18 Sept. 2017, respectively.

Fifty-six lines derived from the CSIRO four-way MAGIC (Multi-parent Advanced Generation Inter-cross) population were

included. The population was developed using the Australian commercial parents Baxter, Chara, Westonia, and Yitpi, each with a low co-ancestry, that were intercrossed to maximize genetic diversity and recombination. A single seed was subsequently selfed to produce pure lines (Huang et al., 2012). These lines were part of a much larger population of almost 1600 lines that were culled to exclude extremes in height and flowering time and then selected for variation in canopy architecture. Selections were based on lines with either erect or floppy upper canopies just before flowering, thus lines varying in light penetration through the flag and penultimate leaves. A further six Australian commercial wheats varying in canopy architecture were also included.

We used a quantum sensor (Li-190R) placed above the canopy to measure daily irradiance ( $i_d$ , the integral of PPFD during a day) above flag leaves, and we placed PARbars below all leaves to measure  $i_d$  below the canopy. PARbars were supported by 2.2-m aluminum square bars that spanned each plot and were supported at either end by gimbals attached to pipe clamps around a polyvinyl chloride (PVC) pipe held in position with a sawhorse positioned in the wheel track between plots (Fig. 4). Bulls-eye levels were used to level the support bars. The quantum sensor was placed atop a 1.6-m angle iron bar attached to a garden cart containing a datalogger (CR5000, Campbell Scientific) and was leveled with a leveling mount. Using relay multiplexers (AM16/32B, Campbell Scientific) enabled us to measure  $i_d$  in 34 plots simultaneously (two ranges of 17 rows) each day. The datalogger and multiplexers were powered with a 12-V deep cycle battery. We set up the datalogger to measure every 10 s continuously throughout the day; the datalogger program (CRBASIC format) is provided in the Supplemental Material (Supplement 3). The equipment was moved southeast to the next pair of ranges after sunset each day. Thus, each plot was measured for one full day at 10-s resolution. Canopy transmittance ( $\tau$ ) was measured as the ratio of below- to above-canopy  $i_d$ .

### Field Setup: California

A standard Californian spring wheat cultivar, Anza, was planted in early December 2017 at the Agriculture Experimental Station UC Davis ( $38^{\circ}31'34''$  N,  $121^{\circ}46'15''$  W). Rows in the experimental field were planted with an approximate true north-south orientation ( $\sim 1.5^{\circ}$  east of north). Measurements were taken on 9, 10, and 11 Mar. 2018 when plant heights ranged between 48 and 51 cm (Zadoks 34, fourth node detectable) (Zadoks et al., 1974). Two Anza plots were spaced adjacent to each other, with one planted as a low-density planting of four rows with 30.48-cm spacing between rows, or double density of seven rows with 15.24-cm between rows. Plots were 6 m long and 91 cm wide, with PARbars shorter than the plot width, so that no active sensing element extended beyond the planted row at the edge of the plot. Plots were separated by 30 cm. PARbars were supported by A-shaped wooden stands and held together with clamps. Each plot had a bar at a 15-cm height and another placed on the soil surface. The plots were measured continuously without moving the PARbars, using a similar datalogger system to the Australia experiment.

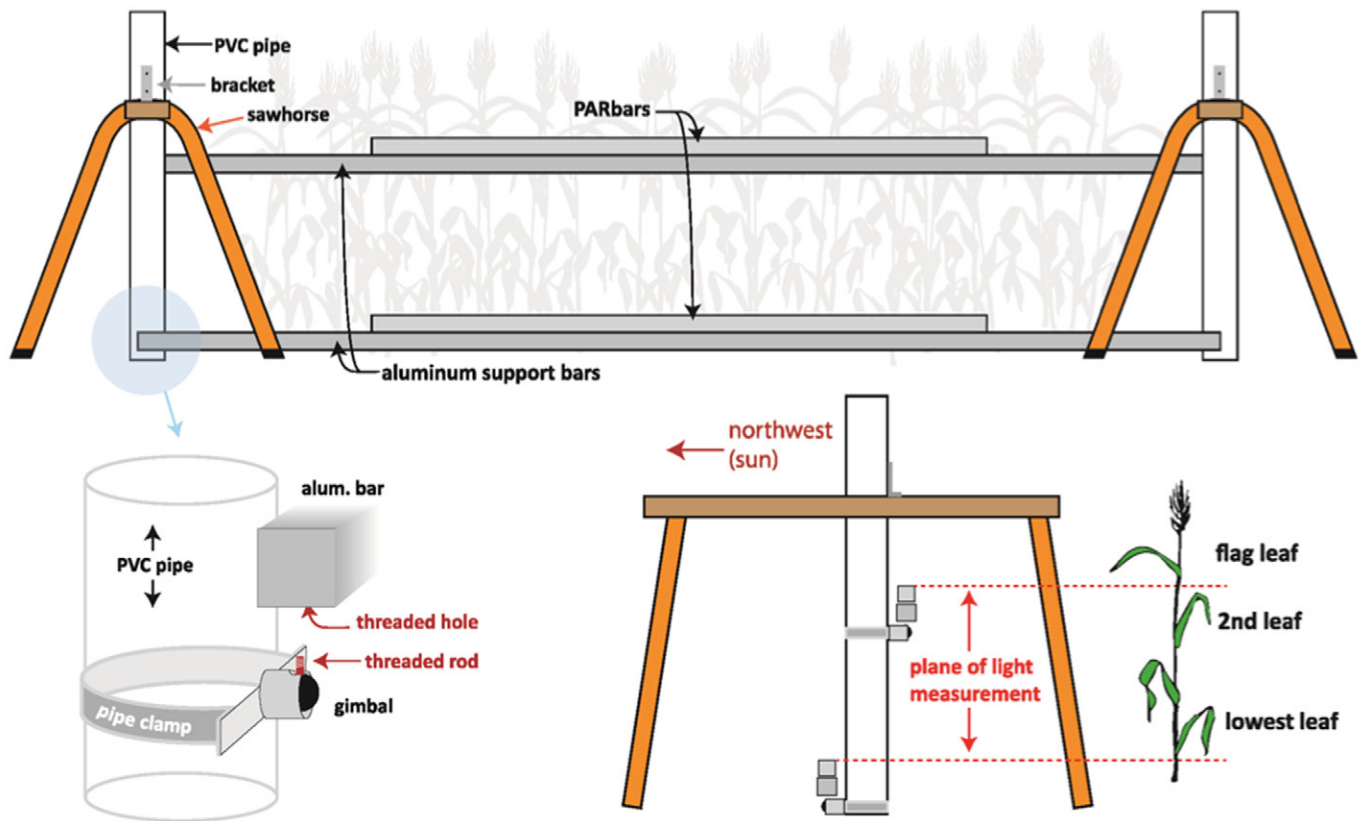


Fig. 4. Placement and mounting mechanisms used to install PARbars in the field in this study: view down the long axis of a field plot, showing sawhorse mounting braces in the between-plot rows at right and left (top); view down the axis of the PARbars themselves, showing orientation of PARbars relative to canopy leaf positions (only data from the lower PARbars shown here were used in the present study) (bottom right); and the mechanism used to mount the aluminum support bars to the vertical PVC pipe posts (bottom left).

### Inference of Effective Plant Area Index

We used equations provided in the manual (Decagon Devices, 2017) for a commonly used commercial ceptometer (AccuPAR LP-80, Decagon Devices) to infer PAI:

$$PAI = \frac{[1 - 1/(2K)]f_b - 1}{A(1 - 0.47f_b)} \ln \tau \quad [1]$$

where  $A = 0.283 + 0.785a - 0.159a^2$ , and  $K$  and  $f_b$  are modeled by Eq. [2] (Campbell, 1986) and Eq. [3] (Decagon Devices, 2009), respectively:

$$K = \frac{(\chi^2 + \tan^2 \theta)^{0.5}}{\chi + 1.744(\chi + 1.182)^{-0.733}} \quad [2]$$

where  $\chi$  is a dimensionless parameter describing the leaf angle distribution ( $\chi$  is the ratio of horizontal to vertical lengths of an ellipsoid whose distribution of surface normal vectors represents the distribution of leaf normal vectors;  $\chi = 1$  for a spherical distribution), and

$$f_b = 1.395 + r \{-14.43 + r[48.57 + r(-59.024 + 24.835r)]\} \quad [3]$$

where  $r$  is PAR above the canopy ( $PAR_{above}$ ) as a fraction of its maximum possible value ( $PAR_{above,max} = 2550 \cos \theta$ ); i.e.,  $r = PAR_{above} / PAR_{above,max}$ . We assumed  $a = 0.9$  and  $\chi = 0.96$  (the latter value was given for wheat by Campbell and Van Evert, 1994).

To estimate the potential impact of a spectral shift beneath canopies on PARbar accuracy, we applied published data for spectral composition across the visible spectrum (measured below wheat canopies at a leaf area index of  $0.65 \text{ m}^2 \text{ m}^{-2}$  and transmittance of 0.73 using a spectral radiometer; Sattin et al., 1994) to the spectral sensitivity of the photodiodes used in our ceptometers. To extrapolate the calculations based on the data from Sattin et al. (1994) to the present study, in which LAI was generally greater and transmittance smaller, we reasoned that the relative spectral shift, and thus the relative error due to imperfect quantum response, should be proportional to the fraction of light absorbed ( $\sim 1 - \text{transmittance}$ ). Thus we estimated the error (%) in PARbar-based transmittance at a given true transmittance ( $\tau$ ) by multiplying the error (%) calculated at  $\tau = 0.73$  from the data of Sattin et al. (1994) by the ratio  $(1 - \tau)/(1 - 0.73)$ .

## Results

### PARbar Ceptometer Calibration

The differential voltage output of our PARbar continuously recording ceptometers was linearly proportional to the output of a reference LI-COR Li-190R quantum sensor (Fig. 3). Calibration slopes for the 68 ceptometers used in Australia averaged  $0.0228 \pm 0.0003 \text{ mV}/(\mu\text{mol m}^{-2} \text{ s}^{-1})$  (mean  $\pm$  SE) and varied with a coefficient of variation of 9.1%; slopes between the four PARbars used in

California varied with a coefficient of variation of 7%. The correlation between PARbar output and LI-COR Li-190R output was  $r^2 > 0.99$  in all cases. Because calibrations differed among PARbars, we suggest that PARbars are not mutually interoperable, and their output must be converted using individual calibrations, like most commercial light sensors including the Li-190R.

### Canopy Transmittance and Inferred Effective Plant Area Index: Australia

Despite apparently constant canopy architecture during a day, canopy PAR transmittance ( $\tau$ ) varied widely during each day for most genotypes, ranging from 0.18 to 0.73 (10th and 90th percentiles, respectively, among readings taken every 10 s in 478 plots of 239 genotypes) diurnally. The value of  $\tau$  was generally greatest in mid-afternoon and mid-morning; the afternoon effect is probably due to alignment of the solar beam with row orientation, whereas the morning effect may result from beam penetration between tillers when the solar beam is roughly perpendicular to rows or from greater penetration of light due to the diffuse fraction of total PAR being greater in the morning. Effective PAI inferred from  $\tau$  using Eq. [1–3], which correct for the influence of solar zenith angle ( $\theta$ ), also varied widely during each day, ranging from 0.44 to 2.24  $\text{m}^{-2}$  (10th and 90th percentiles, respectively). Figure 5 shows 30

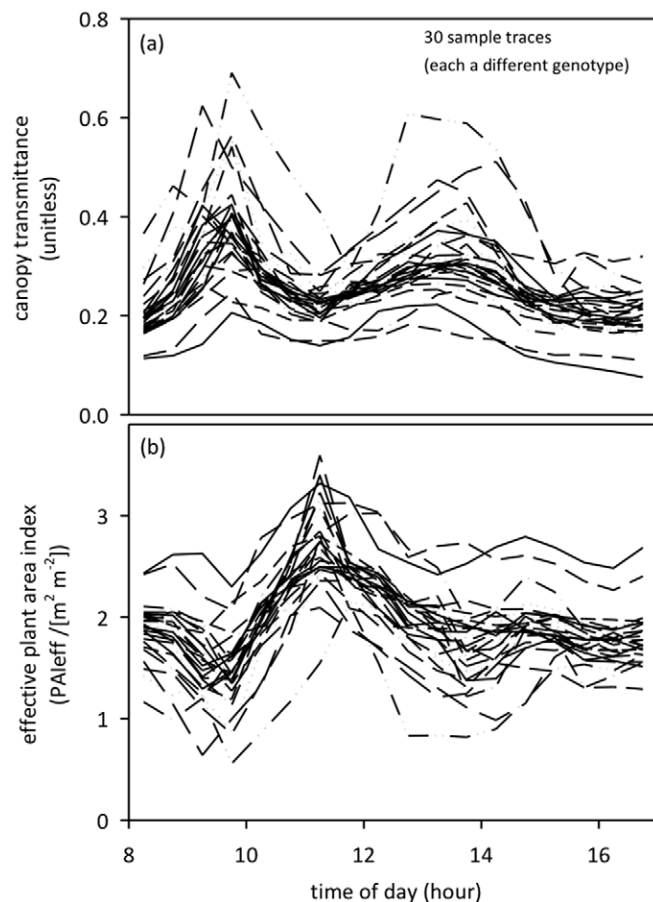


Fig. 5. Sample diurnal traces of measured canopy transmittance ( $\tau$ ) and inferred effective plant area index (PAI) for 30 of the 239 genotypes measured in this study, averaged across 30-min periods.

sample traces for  $\tau$  and PAI (averages of 30-min periods), and Fig. 6 shows medians across genotypes for diurnal traces of  $\tau$  and PAI. The median diurnal average of PAI was 1.84  $\text{m}^{-2}$  (blue line in Fig. 6b).

Thirty-minute averages of PAI inferred from instantaneous ceptometer readings diverged greatly from the diurnal average. Treating the diurnal average inferred PAI for each genotype as its “corrected” PAI, the instantaneous estimates of PAI underestimated the diurnal average PAI by 28% in mid-morning (median across genotypes) and overestimated it by 32% in late morning (Fig. 6c). Across the time window recommended by CIMMYT for instantaneous ceptometer measurements (1100–1400 h) (Pask et al. 2012), the median error ranged from +32 to –11%—a shift equivalent to 43% of the true value. In 10% of genotypes, the error was up to –46% in mid-morning or +61% in late morning (Fig. 6b).

### Canopy Transmittance: California

The California experiment confirmed that time of day, or solar azimuth, plays a role in the observed canopy transmittance. Three consecutive days of partly cloudy, uniformly cloudy, or sunny weather led to contrasting effects on canopy transmittance: the uniformly cloudy day had little variation in transmittance with time (Fig. 7), while the sunny day led to a peak in canopy transmittance at midday. Higher density planting led to smaller diurnal changes in transmittance (Fig. 7c and 7d).

### Relative Error Due to Spectral Shift beneath Canopies

Based on published spectral shifts beneath wheat canopies and the reported spectral sensitivity of our photodiodes (Supplemental Fig. S5), our PARbars would overestimate transmittance by about 2.7% at LAI = 0.65  $\text{m}^{-2}$  (true  $\tau = 0.73$ ), or by 6.1% at  $\tau = 0.4$  and 8.2% at  $\tau = 0.2$ . The difference in these values (2.1%) is the degree to which spectral bias would exaggerate the temporal amplitude in  $\tau$  caused by row orientation and shifting solar azimuth.

## Discussion

Our results show that the time of day at which instantaneous ceptometer measurements are taken can strongly bias measurements of canopy transmittance and inference of PAI. For example, median shifts in PAI across a 3-h midday period were on the order of 40% of the true value for wheat under mostly sunny conditions in early spring in Narrabri, Australia. This represents a potentially large source of uncontrolled and systematic error in canopy properties measured by instantaneous ceptometer. Likewise, the integral of diurnal canopy PAR absorption relates to biomass accumulation and yield potential (Sinclair and Muchow, 1999). Similar errors to those noted for inferred PAI will be introduced by estimating integrated PAR absorption from single ceptometer measurements made at one time of day.

It is important to note that the time-dependent bias reported here did not arise from the effects of solar zenith angle on the canopy extinction coefficient; those effects were accounted for in the calculation of PAI from canopy transmittance (Eq. [1–3]). Instead, they arose from the interaction of solar azimuth with

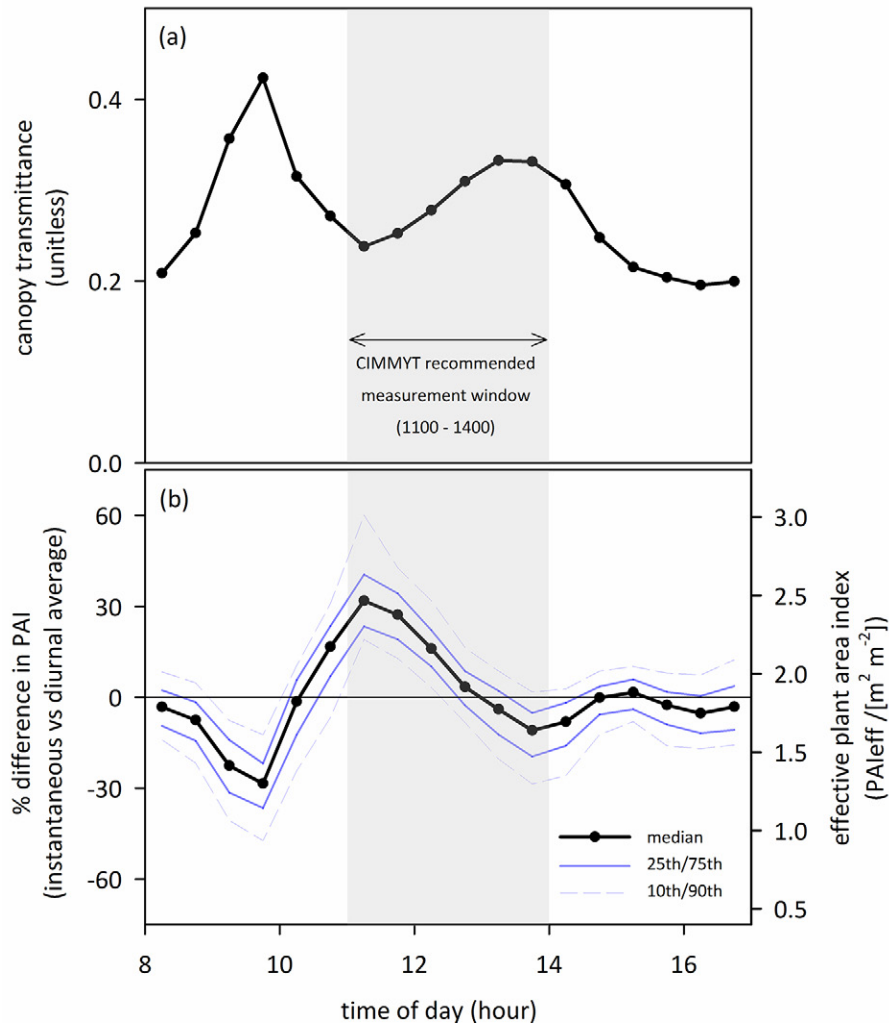


Fig. 6. Median 30-min averages across 239 genotypes of wheat for (a) canopy transmittance ( $\tau$ ), (b) inferred effective plant area index (PAI<sub>eff</sub>, right axis), and the difference between instantaneous PAI<sub>eff</sub> and diurnal average for each genotype (left axis). The blue lines in (b) are percentiles of the error across genotypes. The area shaded gray represents the time window (1100–1400 h) recommended for instantaneous ceptometer measurements in wheat by CIMMYT (Pask et al. 2012).

planting-row orientation, which, as noted earlier by Fuchs and Stanhill (1980), causes large changes in canopy transmittance unrelated to the density of light-absorbing material. In particular, transmittance increases approximately in proportion to the product of the sine of the angle between the row orientation azimuth and solar azimuth ( $\phi$ , Fig. 1) and the tangent of the solar zenith angle ( $\theta$ , Fig. 1) (Fuchs and Stanhill, 1980). Thus, transmittance is enhanced when the solar beam is more nearly aligned with the row orientation; this is evident in Fig. 5a and 6a, which show transmittance peaking in the afternoon, when the solar beam (coming from the north, as the site is in Australia) is approximately aligned with the orientation of our plots ( $44^\circ$  west of true north). In California, the north–south row orientation led to alignment of the plots with the solar beam at midday (Fig. 7).

We emphasize that the specific temporal pattern observed in the Australian data—i.e., inferred PAI peaking in late morning and declining through midday—is particular to the row orientation and geographic location of that study site, and perhaps also to

our study species, wheat. More generally, the exact diurnal timing and magnitude of the row orientation bias in measured transmittance and PAI will depend on aspects of the canopy structure and density that vary widely among crop species and even genotypes, but more importantly, on the row orientation and range of solar zenith angles for a given planting site. For example, the  $44^\circ$  row orientation at our Australian study site is probably not representative of most crop research farms; however, the rows were oriented north–south in the California study and yet we still observed 40 to 50% variation in measured canopy transmittance within 2 h of noon in the low-density planting plots (Fig. 7a and 7b). The zenith angle range varies seasonally and latitudinally; row orientation varies more or less randomly and often reflects historical land use patterns rather than scientific considerations. Leaf angle distribution also varies among genotypes, although we found little differences in the patterns of inferred PAI, or the magnitude of its diurnal range and hence potential temporal bias, for a range of leaf angle distributions (Supplemental Fig. S3). Similarly, plant spacing

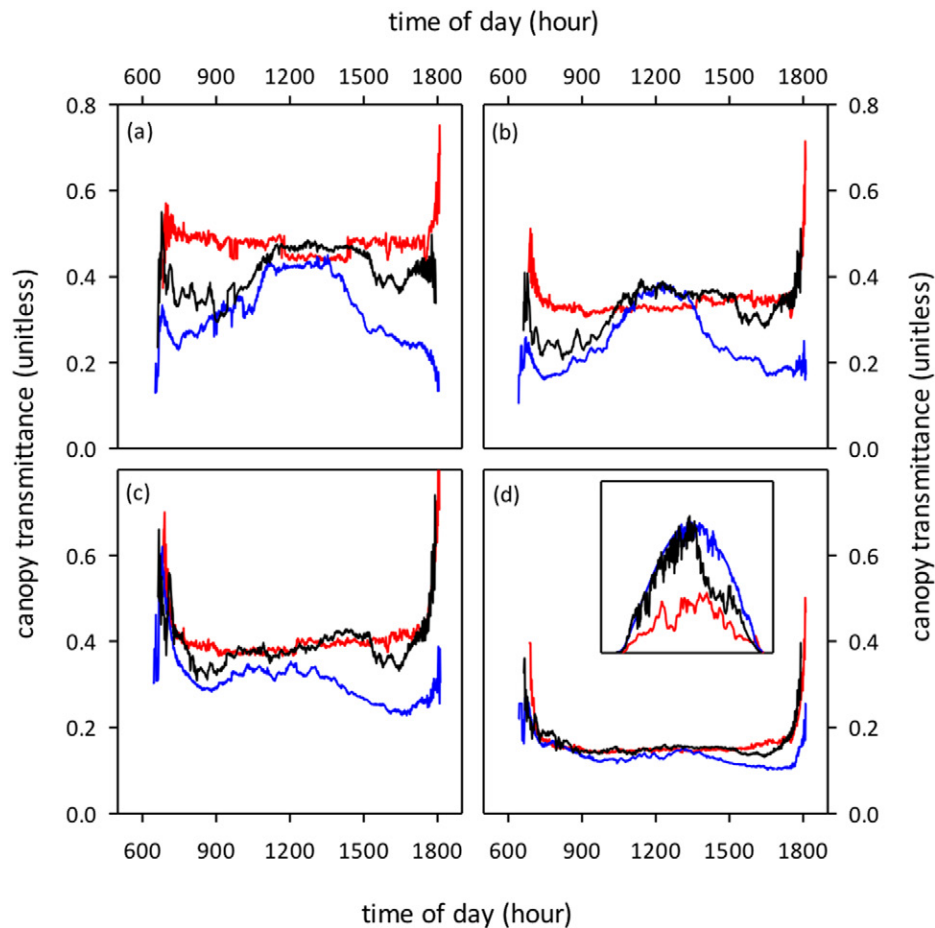


Fig. 7. Diurnal trends in canopy transmittance as measured by PARbars placed at (a,c) mid-canopy or (b,d) on the soil surface in plots of (a,b) low density or (c,d) high density on three consecutive days, with high, moderate, and low photosynthetic photon flux density (blue, black, and red lines, respectively), as shown in the inset figure in (d) (time axis for inset is the same as the larger plots; y axis is  $0\text{--}2000 \mu\text{mol m}^{-2} \text{s}^{-1}$ ). Planting rows were oriented due north–south in a field at the University of California, Davis.

and height will affect the duration of solar alignment with rows independent of other aspects of canopy geometry. A doubling of plant height will halve the duration of solar alignment with rows.

Clumping of vegetation has long been understood to impact the accuracy of PAI or LAI inferred from ceptomety and other methods based on canopy light capture (Lang and Xiang, 1986; Fassnacht et al., 1994; Chen and Cihlar, 1995; Chen et al., 1997; Cohen et al., 1997; White et al., 1997, 2000; Kucharik et al., 1998, 1999; Johnson et al., 2010). When canopy clumping is isotropic (not azimuth dependent), its effect on PAI can be corrected by using an empirical “clumping index” (Chen et al., 2005). However, because row orientation is not isotropic, stationary empirical corrections are inadequate to address the issue raised in this study. Given that the row orientation bias is expected to be reduced when the diffuse fraction of total PAR is greater (in the limiting case of 100% diffuse PAR, row orientation is irrelevant because there is no azimuthal bias in incoming light), one solution would be to take ceptometer measurements only on overcast days (e.g., the cloudy day in Fig. 7, shown with the red line). However, that contrasts with the usual practice and advice, which holds that the ideal conditions for ceptomety are

cloudless skies (e.g., Pask et al., 2012; Decacon Devices, 2017). The spectral distribution of PPFD changes as light is progressively attenuated with increasing optical depth in a canopy, which could also create a bias due to imperfect quantum response in our PARbars. However, our modeling based on observed spectral shifts beneath wheat canopies suggests that this bias would enhance the diurnal amplitude of  $\tau$  caused by the row orientation bias by only around 2%.

We suggest that correction of the row orientation bias under most conditions requires, at a minimum, reliable quantification of the temporal pattern particular to the site and crop in question. That pattern can then be abstracted into a time-dependent empirical correction factor for instantaneous ceptometer measurements. An example of this approach is illustrated in Fig. 8. The median trend in the ratio of diurnal average PAI to instantaneous PAI is modeled using a polynomial function of time within a specific window of time, and this correction function is then calculated at the time of each instantaneous ceptometer measurement and multiplied by that measurement to produce a “corrected” PAI value.

The temporal pattern of row orientation bias can be quantified by repeated instantaneous measurements over time on a few

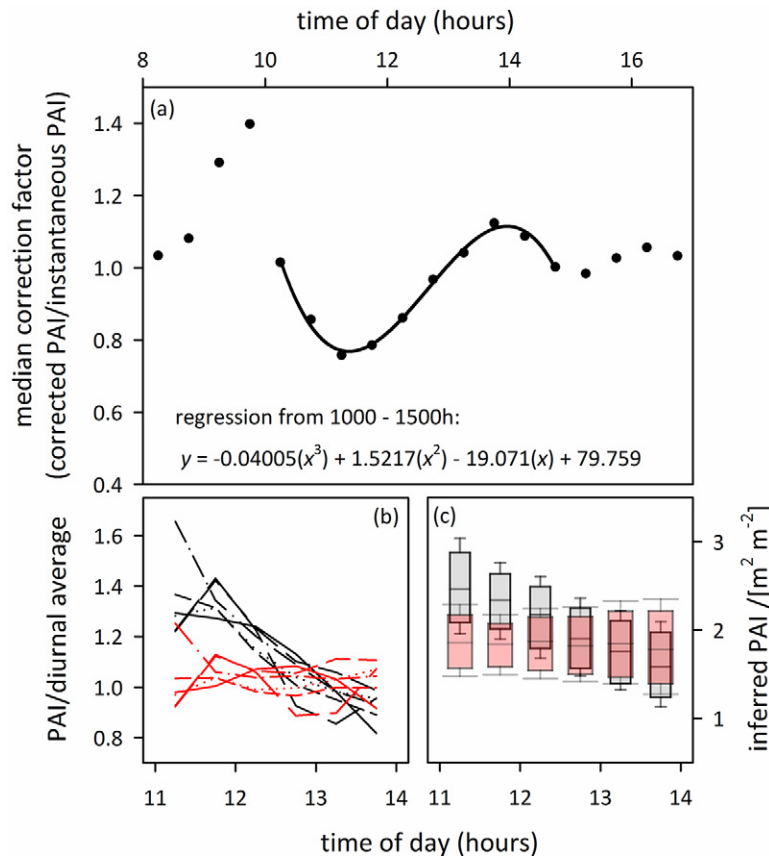


Fig. 8. Example of how a diurnal sequence of ceptometer measurements can be used to correct for the time-dependent bias of row orientation in instantaneous ceptometry: (a) median correction factor (median ratio of diurnal average of inferred plant area index (PAI) to instantaneous value of inferred PAI across 239 genotypes) vs. time of day of instantaneous measurements (30-min averages from continuous [10-s] ceptometer measurements), where the solid line is a third-order polynomial regression ( $r^2 = 0.9923$ ) to the data between 1000 and 1500 h (the equation of this fit is shown on the figure); (b) examples of the ratio of instantaneously inferred PAI to the diurnal average for six plots before (black lines) and after (red lines) correction using the regression from (a); and (c) the distribution of PAI inferred from instantaneous ceptometer measurements across 239 genotypes (midline of box = median; top and bottom of box = 75th and 25th percentiles, respectively; whiskers = 90th and 10th percentiles, respectively) before (gray boxes) and after (red boxes) applying the time-dependent correction shown in (a).

plots, although this is somewhat laborious. Alternatively, one can use continuously recording ceptometers like the PARbars described here to establish the pattern in a number of plots and then apply the result to measurements on other similarly aligned plots in the same general area. Another alternative is to use continuously recording ceptometers for all measurements. Although this has been considered impractical due to the great expense of commercial ceptometers, we showed in this study how PARbars can be constructed with relative ease and low cost ( $\sim$ US\$50 to US\$100 at the time of writing), plus approximately 1 h of labor. Construction of a large number of PARbars would incur a large initial workload but would eliminate the subsequent labor burden of time-intensive instantaneous ceptometer measurements. More importantly, it would also eliminate the row orientation bias discussed in this study.

## Conclusion

Instantaneous ceptometer measurements in row crops are subject to a time-dependent bias caused by diurnal shifts in the alignment of the solar beam with row orientation. This bias cannot be resolved using stationary corrections such as a clumping index.

We recommend that continuously recording ceptometers be used instead of instantaneous ceptometry or that time-explicit ceptometer measurements be used to develop site-specific correction functions to adjust instantaneous measurements for the row orientation bias.

## Acknowledgments

This work was supported by the International Wheat Yield Partnership, via the Grains Research and Development Corporation (US00082) and CIMMYT (IWYP89FP). T.N. Buckley was supported by the Australian Research Council (DP150103863 and LP130100183) and the National Science Foundation (Award no. 1557906). This work was supported by the USDA National Institute of Food and Agriculture, Hatch projects 1016439 and 1001480. Calvin Qualset is thanked for help in planting and Ian Boyles in maintaining the field trial and equipment in California. Julie Lintz is thanked for field assistance in Australia.

## Supplemental Material

Supplement 1: List of materials, costs, and suppliers for manufacture of PARbars.

Supplement 2: Spectral sensitivity of the photodiodes used for PARbars and of another commonly used photodiode in comparison to the ideal sensitivity. Zadoks stages of plants measured in Australia. Effect of leaf angle distribution parameter on inferred PAI trends. Box plots for PAR-

bar calibration parameter distributions. Effect of spectral shift beneath a canopy on transmittance inferred using PARbars.

Supplement 3: CRBASIC datalogger program used to measure PARbar output in Australia.

## References

- Armbrust, D. 1990. Rapid measurement of crop canopy cover. *Agron. J.* 82:1170–1171. doi:10.2134/agronj1990.00021962008200060030x
- Campbell, G.S. 1986. Extinction coefficients for radiation in plant canopies calculated using an ellipsoidal inclination angle distribution. *Agric. For. Meteorol.* 36:317–321. doi:10.1016/0168-1923(86)90010-9
- Campbell, G.S., and F. Van Evert. 1994. Light interception by plant canopies: Efficiency and architecture. In: J.L. Monteith et al., editors, *Resource capture by crops*. Nottingham Univ. Press, Nottingham, UK.
- Chen, J.M., and J. Cihlar. 1995. Plant canopy gap-size analysis theory for improving optical measurements of leaf-area index. *Appl. Opt.* 34:6211–6222. doi:10.1364/AO.34.006211
- Chen, J.M., C.H. Menges, and S.G. Leblanc. 2005. Global mapping of foliage clumping index using multi-angular satellite data. *Remote Sens. Environ.* 97:447–457. doi:10.1016/j.rse.2005.05.003
- Chen, J.M., P.M. Rich, S.T. Gower, J.M. Norman, and S. Plummer. 1997. Leaf area index of boreal forests: Theory, techniques, and measurements. *J. Geophys. Res.* 102(D24):29429–29443. doi:10.1029/97JD01107
- Cohen, S., R.S. Rao, and Y. Cohen. 1997. Canopy transmittance inversion using a line quantum probe for a row crop. *Agric. For. Meteorol.* 86:225–234. doi:10.1016/S0168-1923(96)02426-4
- Decagon Devices. 2009. Application note: Beam fraction calculation in the LP80. Decagon Devices, Pullman, WA
- Decagon Devices. 2017. AccuPAR PAR/LAI Ceptometer Model LP-80 operator's manual. Decagon Devices, Pullman, WA
- Fassnacht, K.S., S.T. Gower, J.M. Norman, and R.E. McMurtric. 1994. A comparison of optical and direct methods for estimating foliage surface area index in forests. *Agric. For. Meteorol.* 71:183–207. doi:10.1016/0168-1923(94)90107-4
- Francone, C., V. Pagani, M. Foi, G. Cappelli, and R. Confalonieri. 2014. Comparison of leaf area index estimates by ceptometer and PocketLAI smart app in canopies with different structures. *Field Crops Res.* 155:38–41. doi:10.1016/j.fcr.2013.09.024
- Fuchs, M., and G. Stanhill. 1980. Row structure and foliage geometry as determinants of the interception of light rays in a sorghum row canopy. *Plant Cell Environ.* 3:175–182.
- Grossman, Y., and T. DeJong. 1998. Training and pruning system effects on vegetative growth potential, light interception, and cropping efficiency in peach trees. *J. Am. Soc. Hortic. Sci.* 123:1058–1064.
- Huang, B.E., A.W. George, K.L. Forrest, A. Kilian, M.J. Hayden, M.K. Morell, and C.R. Cavanagh. 2012. A multiparent advanced generation inter-cross population for genetic analysis in wheat. *Plant Biotech. J.* 10:826–839.
- Johnson, M.V.V., J.R. Kiniry, and B.L. Burson. 2010. Ceptometer deployment method affects measurement of fraction of intercepted photosynthetically active radiation. *Agron. J.* 102:1132–1137. doi:10.2134/agronj2009.0478
- Kucharik, C.J., J.M. Norman, and S.T. Gower. 1998. Measurements of branch area and adjusting leaf area index indirect measurements. *Agric. For. Meteorol.* 91:69–88. doi:10.1016/S0168-1923(98)00064-1
- Kucharik, C.J., J.M. Norman, and S.T. Gower. 1999. Characterization of radiation regimes in nonrandom forest canopies: Theory, measurements, and a simplified modeling approach. *Tree Physiol.* 19:695–706. doi:10.1093/treephys/19.11.695
- Lang, A.R.G., and Y. Xiang. 1986. Estimation of leaf area index from transmission of direct sunlight in discontinuous canopies. *Agric. For. Meteorol.* 37:229–243. doi:10.1016/0168-1923(86)90033-X
- López-Lozano, R., F. Baret, I.G. de Cortazar-Atauri, N. Bertrand, and M.A. Casterad. 2009. Optimal geometric configuration and algorithms for LAI indirect estimates under row canopies: The case of vineyards. *Agric. For. Meteorol.* 149:1307–1316. doi:10.1016/j.agrformet.2009.03.001
- López-Lozano, R., and M.A. Casterad. 2013. Comparison of different protocols for indirect measurement of leaf area index with ceptometers in vertically trained vineyards. *Aust. J. Grape Wine Res.* 19:116–122. doi:10.1111/ajgw.12005
- Pask, A., J. Pietragalla, D. Mullan, and M. Reynolds. 2012. Physiological breeding II: A field guide to wheat phenotyping. CIMMYT, Mexico.
- Pearcy, R.W., J.S. Roden, and J.A. Gamon. 1990. Sunfleck dynamics in relation to canopy structure in a soybean (*Glycine max* (L.) Merr.) canopy. *Agric. For. Meteorol.* 52:359–372. doi:10.1016/0168-1923(90)90092-K
- Rosenthal, W., and T. Gerik. 1991. Radiation use efficiency among cotton cultivars. *Agron. J.* 83:655–658. doi:10.2134/agronj1991.00021962008300040001x
- Sattin, M., M.C. Zuin, and I. Sartorato. 1994. Light quality beneath field-grown maize, soybean and wheat canopies: Red:far red variations. *Physiol. Plant.* 91:322–328. doi:10.1111/j.1399-3054.1994.tb00439.x
- Sinclair, T.R., and R.C. Muchow. 1999. Radiation use efficiency. *Adv. Agron.* 65:215–265. doi:10.1016/S0065-2113(08)60914-1
- Webb, N., C. Nicholl, J. Wood, and E. Potter. 2016. User manual for the SunScan Canopy Analysis System Type SS1. Delta-T Devices, Cambridge, UK
- Welles, J.M. 1990. Some indirect methods of estimating canopy structure. *Remote Sens. Rev.* 5(1):31–43. doi:10.1080/02757259009532120
- Whaley, J., D. Sparkes, M. Foulkes, J. Spink, T. Semere, and R. Scott. 2000. The physiological response of winter wheat to reductions in plant density. *Ann. Appl. Biol.* 137:165–177. doi:10.1111/j.1744-7348.2000.tb00048.x
- White, J.D., S.W. Running, R. Nemani, R.E. Keane, and K.C. Ryan. 1997. Measurement and remote sensing of LAI in Rocky Mountain montane ecosystems. *Can. J. For. Res.* 27:1714–1727. doi:10.1139/x97-142
- White, M.A., G.P. Asner, R.R. Nemani, J.L. Privette, and S.W. Running. 2000. Measuring fractional cover and leaf area index in arid ecosystems: Digital camera, radiation transmittance, and laser altimetry methods. *Remote Sens. Environ.* 74:45–57. doi:10.1016/S0034-4257(00)00119-X
- Zadoks, J.C., T.T. Chang, and C.F. Konzak. 1974. A decimal code for the growth stages of cereals. *Weed Res.* 14:415–421.